New Schemes for Confinement of Fusion Products in Stellarators

W.A. Cooper 2), M.Yu. Isaev 1), M.F. Heyn 5), V.N. Kalyuzhnyj 3), S.V. Kasilov 3), W. Kernbichler 5), A.Yu. Kuyanov 1), M.I. Mikhailov 1), V.V. Nemov 3), J. Nührenberg 4), M.A. Samitov 1), V.D. Shafranov 1), A.A. Skovoroda 1), A.A. Subbotin 1), R. Zille 4), A.V. Zvonkov 1)

1) Russian Research Centre "Kurchatov Institute", Moscow, Russia
2) Centre de Recherches en Physique des Plasmas, Association Euratom-Confédération Suisse, Ecole Polytechnique Fédérale de Lausanne, Switzerland
3) Institute of Plasma Physics, National Science Center "Kharkov Institute of Physics and Technology", Kharkov, Ukraine
4) Max-Planck-Institut für Plasmaphysik, IPP-EURATOM Association, Germany
5) Institut für Theoretische Physik, Technische Universität Graz, Graz, Austria

Abstract. Improved energetic-particle confinement is found in new stellarator and toroidal mirror field configurations. The possibility of fulfilling the condition of poloidal closure of the contours of the second adiabatic invariant for all reflected particles is studied for stellarators with poloidally closed contours of the magnetic field *B* on the magnetic surfaces through computational stellarator optimization. It is shown that by adjusting the geometry this is possible in a major fraction of the plasma volume. The most salient characteristic (as compared to previous quasi-isodynamic configurations) is a magnetic axis whose curvature vanishes in all cross-sections with an extremum of *B* on the magnetic axis and renders possible a 3D structure of *B* with unprecedently high collisionless α-particle confinement. Sectionally isometric vacuum magnetic field toroidal mirror traps are analytically constructed with the help of the paraxial (or 'thin tube') approximation. Application of standard computational stellarator tools to this type of $\iota = 0$ stellarator shows excellent alignment of second adiabatic invariant contours and equilibrium surfaces as well as directly calculated collisionless confinement of energetic particles.

1. Introduction

In this paper two qualitatively new schemes for perfect confinement of the collisionless orbits of energetic particles are described. The first one is a stellarator configuration of quasi-isodynamic [1] type with the special property of non-existence of reflected particles not localized to periods of the configuration. The second one is a toroidal mirror trap designed with the principle of isometry [2] which entails the contours of the second adiabatic invariant to coincide with magnetic surfaces.

2. Stellarator Configuration

Quasi-helically symmetric and quasi-axisymmetric stellarators in which *B* is two-dimensional in magnetic coordinates to such a high degree in truly 3d configurations that collisionless particle confinement is sufficiently improved were found by stellarator optimization. Poloidal quasi-symmetry cannot be satisfied in toroidal stellarators; the improvement of collisionless particle confinement in systems attempting a nearly equivalent substitute for this missing quasi-symmetry can be achieved by direct optimization of collisionless orbit behaviour. For *deeply to moderately deeply reflected* particles this is equivalent to optimization of the contours of the second adiabatic invariant to be constant on magnetic surfaces. Collisionless diffusion of *barely reflected* particles constitutes the residual loss in systems found previously, in which the magnetic axis has maximum curvature in the region of maximum *B*, so that the contours of *B* on magnetic surfaces are not poloidally closed, i.e. form 'islands' in this region. The condition of pseudo-symmetry [3] is necessary to avoid this situation.

Therefore, as an initial condition a nearly pseudo-symmetric configuration is used for the optimization which then can be done without long-time following of guiding centre orbits but with targeting poloidal closure of the contours of the second adiabatic invariant. It is shown that this is possible in a major fraction of the plasma volume and results in excellent energetic-particle confinement. Figure 1 shows the result of such an optimization of a stellarator with six periods.

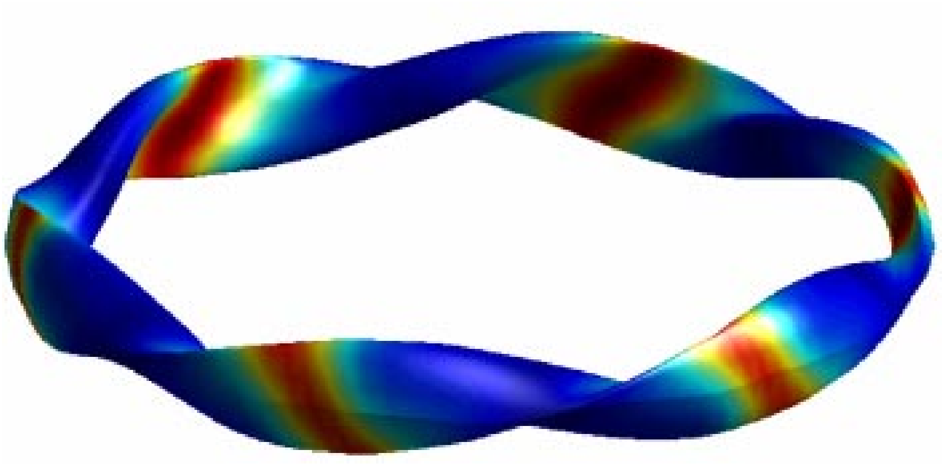

FIG. 1. Boundary magnetic surface of the optimized configuration also showing the magnetic topography. The colors define the range of the magnetic field strength (red - maximum, blue - minimum, $(B_{max}-B_{min})/B \approx 0.5$). The characteristic feature of the configuration is the nearly vanishing curvature of the plasma column in the regions of the extrema of B.

Figure 2 (left) shows on the one hand that the condition of pseudo-symmetry is only slightly violated as seen from the small residual 'island' in the B contours near the maximum of B and, on the other hand, qualitatively, the geometry of the poloidally closed contours which renders the second adiabatic invariant nearly constant. Figure 2 (right) shows contours of B in 3d which exhibit the absolute minimum of B at the minimum of B along the axis and the geometric reason for the maximum-ϑ property: the reflection surfaces bounding the constant-ϑ orbits are concave as viewed from the trajectory region. Finally, Figure 3 shows the alignment of the ϑ contours with the magnetic surfaces and the ensuing excellent collisionless confinement of fusion protons.

3. Toroidal mirror trap

The toroidal mirror trap is studied with a combination of analytical and computational methods. Boozer coordinates (Φ, θ, ζ) are used, where Φ is the toroidal flux and, in a configuration with closed field lines, θ labels the magnetic field line on the magnetic surface; for a vacuum field ζ coincides with the scalar magnetic potential. The components of the metric tensor in Boozer coordinates must satisfy the conditions

$$g_{13} = g_{23} = 0, \qquad g_{11}g_{22} - g_{12}^2 = g_{33}/F^2,$$

where F is the poloidal current. The isometry condition implies equal lengths of magnetic field lines between any two contours $B = const$ on the magnetic surface and has the form [2]

$$\partial g_{33}/\partial\theta = f \partial g_{33}/\partial\zeta,$$

where ϕ is a bounded function of Φ, θ, periodic in θ. The condition of weak isometry implies equal lengths of magnetic field lines between two contours $B = const$ with the same B value;

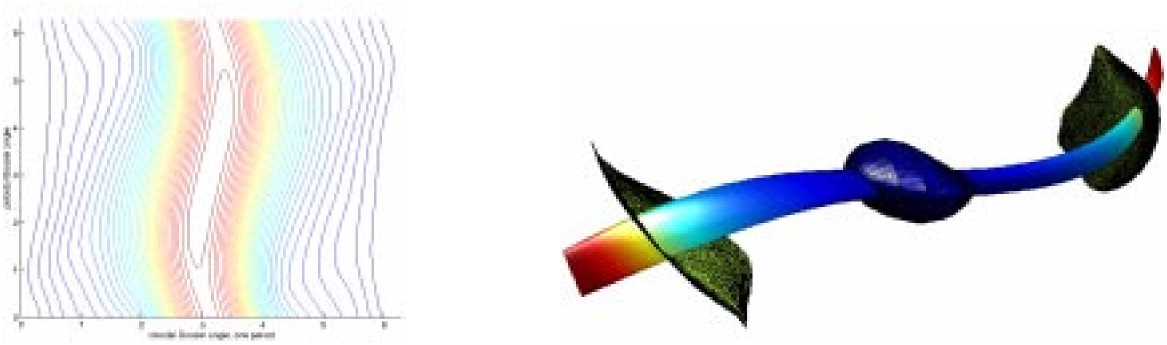

FIG. 2. Left: The contours of B on the magnetic surface at half of the minor plasma radius. It is seen that a small residual local maximum of B still exists.
Right: Near axix magnetic surface and three contours of B, two open ones and one topologically spherical one which encloses the minimum of B.

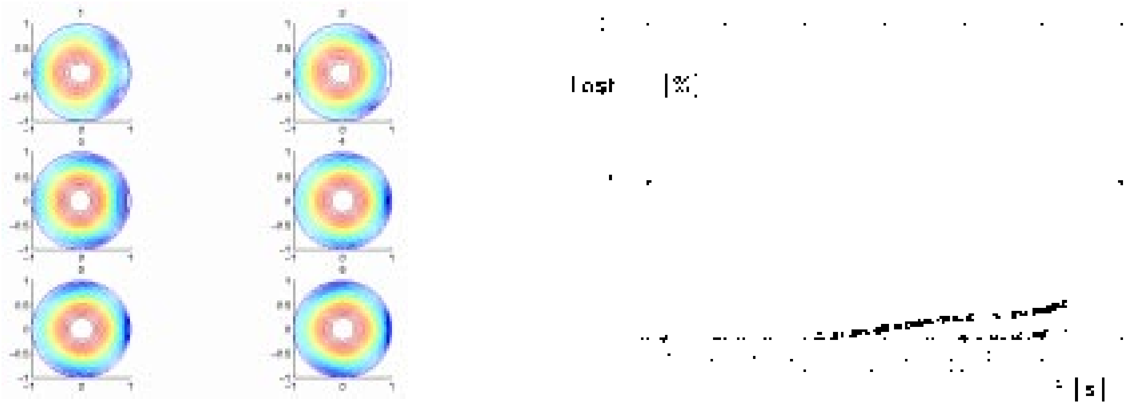

FIG. 3. Left: ϑ for increasing values of B_{ref} in polar-coordinate representation $\sqrt{s}$, θ with s the flux label. Labels i = 1, ..., 6: $B_{ref} = B_{min} + i\Delta B/7$. The red color corresponds to the maximal value of ϑ showing the maximum-ϑ property of this configuration.
Right: Collisionless fast-particle losses of the configuration shown in Figure 1. Eight hundred 14.7 MeV protons are started at 0.5 and 0.7 of the plasma radius and followed in a device with 10^3 m^3 and 5 T. Each symbol indicates the loss of one particle at the time of its loss and the percentage lost to this time.

this can be stated as $B = B(\Phi, \zeta + \lambda(\Phi, \theta, B))$. From this relationship the above equation can be derived, where ϕ is now a function of Φ, θ, B. The fulfilment of the conditions of isometry or weak isometry entails the equilibrium

$$\oint dl / B = U(\Phi)$$

and exact omnigeneity, that is the absence of superbanana drift orbits.
An up-down symmetric vacuum magnetic configuration is considered near the magnetic axis that is a plane curve with variable curvature. To ensure the field line closure, a magnetic configuration having reflection symmetry with respect to some plane, e.g. $y = 0$ is selected. In a paraxial approximation, the coordinates of the magnetic surface can be expanded near the axis as

$$x = x_{axis} - \sqrt{\Phi}a\left(\cos\theta + \sqrt{\Phi}(\Delta_0 + \Delta_1\cos 2\theta)\right)\sin\alpha + \Phi\Sigma\cos\alpha,$$
$$y = y_{axis} + \sqrt{\Phi}a\left(\cos\theta + \sqrt{\Phi}(\Delta_0 + \Delta_1\cos 2\theta)\right)\cos\alpha + \Phi\Sigma\sin\alpha,$$
$$z = \sqrt{\Phi}b\left(\sin\theta + \sqrt{\Phi}\Gamma\sin 2\theta\right)$$

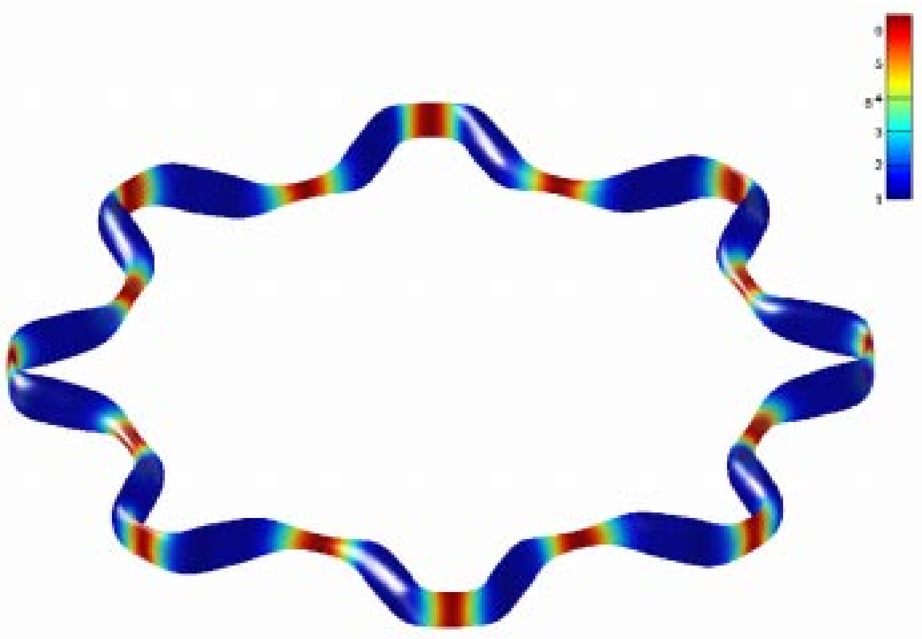

FIG. 4. Boundary magnetic surface of eight-period trap. Dimensionless parameters: aspect ratio 20.65, mirror ratio 5.84, major radius min/max 0.75, ‹ β › 0.1%; the α-particle confinement (see Fig. 6) is assessed with device dimensions: plasma volume 469.5m^3 (corresponding to a volume-averaged minor radius 1.114m) and average magnetic field 5T.

where α is the axis tangent angle. The conditions of the first [2] and the second order [4,5] for both isometry and weak isometry are

$$k = 2C_1(ab)'/Fa^2b,$$

$$a(a'/ab)' - b(b'/ab)' = -(C_1^2(ab)')' + F(C_2 - 4C_1\Delta_1)(ab)'/2,$$

where k is the axis curvature and prime denotes the derivative with respect to the toroidal coordinate ζ. In case of isometry C_1 and C_2 are constants, whereas for weak isometry they are functions of ab. The configuration is determined by the solution of these equations, for details see [5]. In the isometric case C_1 is taken positive in one halfperiod, and negative, namely $-C_1$, in the other one. The change of sign takes place in the maximum of the magnetic field where $(ab)' = 0$; hence the curvature is a continuous function. For simplicity $C_2 = \Delta_1 = 0$ are used. Fig. 4 represents the boundary magnetic surface for such an eight-period toroidal mirror trap. The boundary surface was used as input for the VMEC, JMC, MCT code chain. The modeling confirmed that the contours of

$$\oint dl / B$$

coincide well with the calculated equilibrium magnetic surfaces for $\beta = 0.1\%$. The contours of B on a magnetic surface are shown in Fig. 5, left, and in a 3D view in its right part. Because the configuration is only sectionally isometric, a small violation of isometry can be seen. The contours of the second adiabatic invariant ϑ coincide well with the equilibrium magnetic surfaces, as seen in Fig. 6, left, which means that the omnigeneity condition is fulfilled for almost all trapped particles. The collisionless orbits of 3.6 MeV α-particles for reactor-like parameters (see Fig. 4) are illustrated by Fig. 6, right, where the particle loss from two magnetic surfaces is shown.

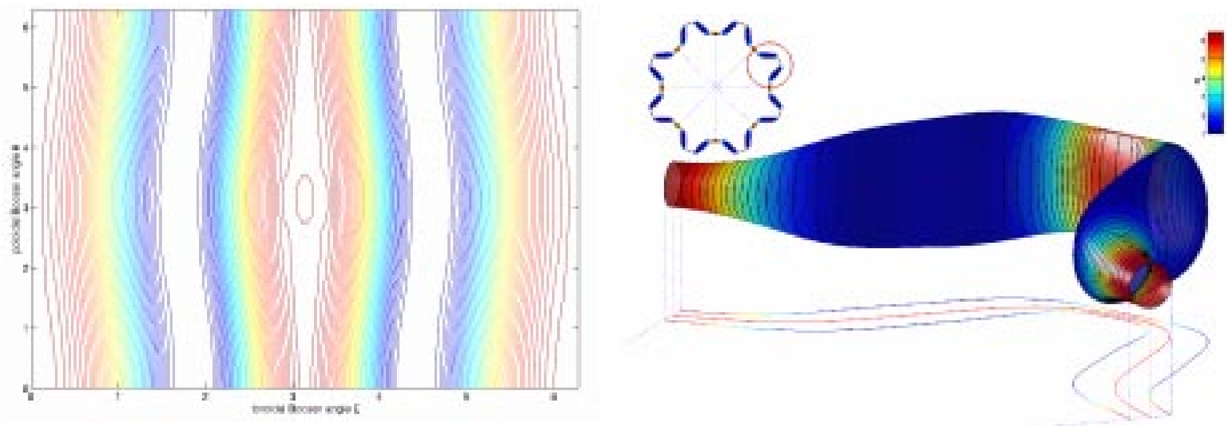

FIG. 5. Contours of B on a magnetic surface, and boundary as well as midplane field lines of one field period.

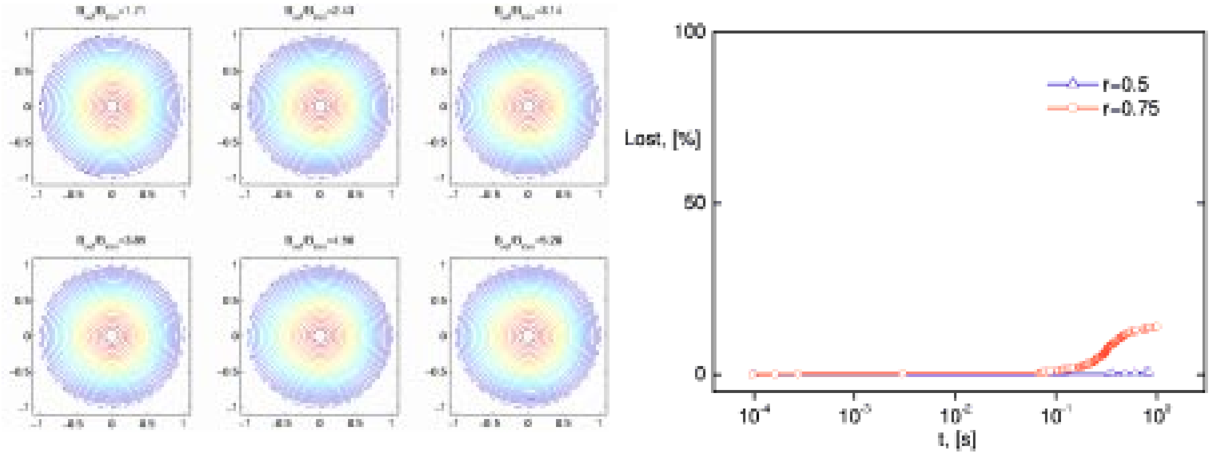

FIG. 6. Alignment of magnetic and ϑ surfaces as well as collisionless confinement of α-particles

4. Conclusions

For both types of configurations, the stellarator configuration without transitional particles and the isometric toroidal mirror trap, further investigations are envisaged. For the stellarator, by way of example, Mercier stabililty prevails at $<\beta> = 0.05$ but a more elaborate MHD stability analysis remains to be done. For the mirror trap, again by way of example, the case of weak isometry is already being investigated and finite-β configurations have to be determined.

This work was supported by INTAS Grant No 99-00592, by the Russian-Germany agreement WTZ-V RUS-563-98 and WTZ RUS-01-581, by the Russian Federal program on support of leading scientific schools, Grant No 00-15-96526, by the Russian Fund for Basic Research, Grant No 00-02-17105, and by the Fonds National Suisse de la Recherche Scientifique and Euratom.

5. References

[1] GORI, S., et al., Theory of Fusion Plasmas, Bologna: SIF (1996) 335.
[2] SKOVORODA, A.A., Shafranov V.D., Plasma Physics Rep. 21 (1995) 937.
[3] MIKHAILOV, M.I. et al., Theory of Fusion Plasmas, Bologna: SIF (1998) 185.
[4] ARSENIN, V.V. et al., Nucl. Fusion 41 (2001) 945.
[5] ZVONKOV, A.V. et al., Plasma Physics Rep. 28 (2002) 756.